

Pnictogen-bridged antiferromagnetic superexchange interactions in iron pnictides

Zhong-Yi Lu^{1,*}, Fengjie Ma^{1,3}, and Tao Xiang^{2,3†}

¹*Department of Physics, Renmin University of China, Beijing 100872, China*

²*Institute of Physics, Chinese Academy of Sciences, Beijing 100190, China and*

³*Institute of Theoretical Physics, Chinese Academy of Sciences, Beijing 100190, China*

(Dated: June 30, 2010)

The first-principles electronic structure calculations made substantial contribution to study of high T_c iron-pnictide superconductors. By the calculations, LaFeAsO was first predicted to be an antiferromagnetic semimetal, and the novel bi-collinear antiferromagnetic order was predicted for α -FeTe. Moreover, based on the calculations the underlying mechanism was proposed to be Arsenic-bridged antiferromagnetic superexchange interaction between the next-nearest neighbor Fe moments. In this article, this physical picture is further presented and discussed in association with the elaborate first-principles calculations on LaFePO. The further discussion of origin of the magnetism in iron-pnictides and in connection with superconductivity is presented as well.

I. INTRODUCTION

Since the discovery of superconductivity in LaFeAsO by partial substitution of O with F atoms below 26K [1], intense studies have been devoted to physical properties of iron-based pnictides both experimentally and theoretically. Unlike study of the cuprates, the first-principles electronic structure calculations made substantial contribution to study of the pnictides from the very beginning. By the calculations, we first predicted that LaFeAsO is an antiferromagnetic semimetal [2], and then predicted that the ground state of α -FeTe is in a novel bi-collinear antiferromagnetic order [3]. These predictions were confirmed by the later neutron scattering experiments [4, 5]. Moreover, based on the calculations, we proposed [6] the fluctuating Fe local moments with the As-bridged antiferromagnetic superexchange interaction to account for the magnetism and tetragonal-orthorhombic structural distortion in LaFeAsO.

There are, so far, four types of iron-based compounds reported, showing superconductivity after doping or under high pressures, i.e., 1111-type $ReFeAsO$ (Re = rare earth) [1], 122-type AFe_2As_2 (A =Ba, Sr, or Ca) [7], 111-type $BFeAs$ (B = alkali metal) [8], and 11-type tetragonal α -FeSe(Te) [9]. Like cuprates, all these compounds have a layered structure, namely they share the same structural feature that there exist the robust tetrahedral layers where Fe atoms are tetragonally coordinated by pnictogen or chalcogen atoms and the superconduction pairing may happen. A universal finding is that all these compounds are in a collinear antiferromagnetic order below a tetragonal-orthorhombic structural transition temperature [4, 10] except for α -FeTe that is in a bi-collinear antiferromagnetic order below a tetragonal-triclinic structural transition temperature [3, 5, 11].

The above finding raises the question on the microscopic mechanisms underlying the structural transition

and antiferromagnetic transition respectively and the relationship between these two transitions. There are basically two contradictive views upon this question. The first one [12] is based on itinerant electron picture, which thinks that there are no local moments and the collinear antiferromagnetic order is induced by the Fermi surface nesting which is also responsible for the structural transition due to breaking the four-fold rotational symmetry. On the contrary, the second one is based on local moment picture. The J_1 - J_2 Heisenberg model was, phenomenologically [13] and from strong electron correlation limit [14] respectively, proposed to account for the issue. Meanwhile, we proposed [6] the fluctuating Fe local moments with the As-bridged antiferromagnetic superexchange interactions as the driving force upon the two transitions, effectively described by the J_1 - J_2 Heisenberg model as well.

Our proposal embodies the twofold meanings shown by the calculations [6]: (1) there are localized magnetic moments around Fe ions and embedded in itinerant electrons in real space; (2) it is those bands far from the Fermi energy rather than the bands nearby the Fermi energy that determine the magnetic behavior of pnictides, namely the hybridization of Fe with the neighbor As atoms plays a substantial role. Here the formation of local moment on Fe ion is mainly due to the strong Hund's rule coupling on Fe 3d-orbitals [6]. In this sense, our proposal can be considered as the Hund's rule correlation picture. We emphasize again that the Arsenic atoms play a substantial role in our physical picture. Subsequently we successfully predicted from the calculations [6], based on this Hund's rule correlation picture, that the ground state of α -FeTe is in a bi-collinear antiferromagnetic order, which was later confirmed by the neutron scattering experiments [5, 11].

Here we would like to address that our physical picture works well on all iron-based pnictide superconductors, including LaFePO. In this article, we will show how our physical picture works on LaFePO through the elaborate first-principles electronic structure calculations. We find that there is P-bridged next-nearest neighbor Fe-Fe superexchange antiferromagnetic interaction while the

*Electronic address: zlu@ruc.edu.cn

†Electronic address: txiang@aphy.iphy.ac.cn

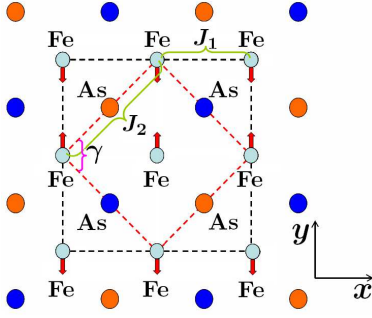


FIG. 1: (Color online) Schematic top view of the FeAs or FeP layer in LaFeAsO or LaFePO. The small dashed square is an $a \times a$ unit cell while the large dashed square is a $\sqrt{2}a \times \sqrt{2}a$ unit cell. The Fe-spins are aligned in a collinear antiferromagnetic order.

nearest neighbor Fe-Fe exchange interaction is very small in LaFePO. This results in the collinear antiferromagnetic order of Fe moments in the ground state, similar to the scenario in LaFeAsO. Moreover, we demonstrate that there also exists a small monoclinic lattice distortion resulting from this superexchange magnetic interaction, again similar to the one in LaFeAsO [6].

II. COMPUTATIONAL APPROACH

In the calculations the plane wave basis method was used [15]. We used the generalized gradient approximation (GGA) of Perdew-Burke-Ernzerhof [16] for the exchange-correlation potentials. The ultrasoft pseudopotentials [17] were used to model the electron-ion interactions. After the full convergence test, the kinetic energy cut-off and the charge density cut-off of the plane wave basis were chosen to be 600eV and 4800eV, respectively. The Gaussian broadening technique was used and a mesh of $16 \times 16 \times 8$ k-points were sampled for the Brillouin-zone integration. In the calculation, the internal atomic coordinates within the cell were determined by the energy minimization.

The crystal structure of LaFePO belongs to the tetragonal structure and the space group is of P4/nmm. In the calculations, we adopted two unit cells, namely $a \times a \times c$ crystal unit cell and $\sqrt{2}a \times \sqrt{2}a \times c$ unit cell respectively, as shown in Fig. 1. Here we used the experimental lattice parameters with $a=3.964 \text{ \AA}$ and $c=8.512 \text{ \AA}$. We also checked the results with the optimized lattice parameters ($a=b=3.932 \text{ \AA}$, $c=8.415 \text{ \AA}$) and there is no significant change found.

III. RESULTS AND ANALYSIS

In order to derive the exchange interactions between the Fe-Fe moments, we designed three different magnetic structures, including the nonmagnetic, the ferro-

magnetic, and the checkerboard (Neel) antiferromagnetic structures calculated in $a \times a \times c$ crystal unit cell, and the collinear antiferromagnetic structure calculated in $\sqrt{2}a \times \sqrt{2}a \times c$ unit cell. The calculations show that the energy differences among the nonmagnetic, the ferromagnetic, and the checkerboard antiferromagnetic states are so small that these three states can be considered as degenerate, similar to the ones in Ref. [18]. The calculated electronic band structure and the Fermi surface are also the same as the ones in the previous calculations [18, 19]. From the volumes enclosed by the Fermi surface sheets, we derive that both hole and electron carrier density is about $2.75 \times 10^{21}/\text{cm}^3$. Thus LaFePO in the nonmagnetic phase behaves as a semimetal. However, the calculation upon the collinear antiferromagnetic structure in LaFePO shows that the ground state of LaFePO is of the collinear antiferromagnetic ordering on the Fe moments. The energy of the collinear antiferromagnetic ordered state is about 33 meV per formula unit cell lower than the nonmagnetic one. The magnetic moment around each Fe atom is found to be nearly $2.0\mu_B$, smaller than the one in the calculation on LaFeAsO [6].

These magnetic states can be modeled by the following frustrated Heisenberg model with the nearest and next-nearest neighbor couplings J_1 and J_2

$$H = J_1 \sum_{\langle ij \rangle} \vec{S}_i \cdot \vec{S}_j + J_2 \sum_{\langle\langle ij \rangle\rangle} \vec{S}_i \cdot \vec{S}_j, \quad (1)$$

whereas $\langle ij \rangle$ and $\langle\langle ij \rangle\rangle$ denote the summation over the nearest and next-nearest neighbors, respectively. From the calculated energy data, we find that $J_1 \sim 0.5 \text{ meV}/S^2$ and $J_2 \sim 7.5 \text{ meV}/S^2$. If the spin of each Fe ion $S = 1$, then $J_1 \sim 0.5 \text{ meV}$ and $J_2 \sim 7.5 \text{ meV}$ (The detailed calculation is referred to Appendix of Ref. 6). In comparison with LaFeAsO [6], the J_1 and J_2 are smaller by 7 times for LaFePO.

Fig. 2 (a) and (b) show the calculated charge distributions on the (001) plane crossing four Fe atoms and the plane (110) crossing Fe-P-Fe atoms, respectively. We see that there is a strong bonding between Fe and P ions. This indicates that the next-nearest neighbor coupling J_2 is induced by the superexchange bridged by P $3p$ -orbitals. This superexchange is antiferromagnetic because the intermediated state associated with the virtual hopping bridged by P ions is a spin singlet. The charge distribution between the two nearest Fe ions is finite but almost none between the next-nearest Fe ions. Thus there is a direct exchange interaction between the two nearest neighboring Fe spins. Because of the exists of the strong Hund's coupling induced direct ferromagnetic exchange interaction and the indirect antiferromagnetic superexchange interaction bridged by P $3p$ -orbitals, combined with the degeneration of different magnetic states in $a \times a \times c$, the nearest neighbor coupling J_1 is nearly zero.

For the collinear antiferromagnetic structure, our calculations show that there is further small structural distortion that shrinks along the spin-parallel alignment (x-

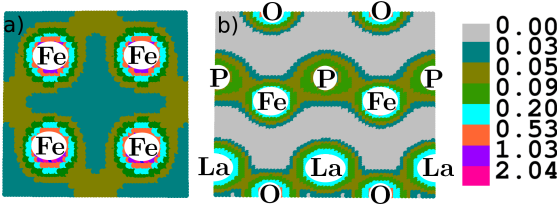


FIG. 2: (Color online) Calculated charge density distribution of LaFePO in the (001) plane crossing Fe-Fe atoms (a) and in the (110) plane crossing Fe-P-Fe atoms (b).

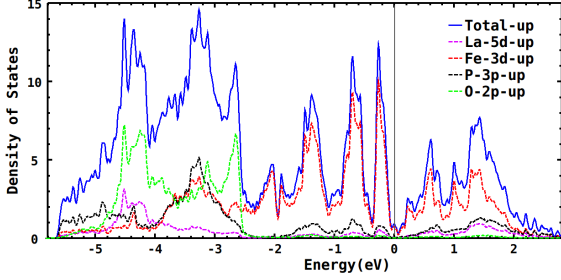


FIG. 3: (Color online) Calculated total and orbital-resolved partial density of states (spin-up part) of LaFePO in the collinear antiferromagnetic state. The Fermi energy is set to zero.

axis in Fig. 1) and expands along the spin-antiparallel alignment (y-axis in Fig. 1), causing structural transition from tetragonal structure to monoclinic structure. This is easily understandable that the direct exchange favors a shorter Fe-Fe separation while the superexchange favors a larger Fe-P-Fe angle. It turns out that the angle γ in ab-plane (see Fig. 1) is no longer rectangular and optimized to be 90.57° with a small energy gain of about 3meV, similar to the finding in LaFeAsO [6]. Such a small distortion is found to have a small effect upon the electronic structure and the Fe moments. Here we emphasize that our calculations show that the driving force upon this structural distortion is nothing but the magnetic interaction. More specifically it is the superexchange interaction J_2 that breaks the rotational symmetry to induce both the structural distortion and the Fe-spin collinear antiferromagnetic ordering.

Fig. 3 shows the total and projected density of states of LaFePO in the collinear antiferromagnetic state. The most of the states around the Fermi level are of Fe 3d characters. The corresponding electronic density of states is 1.45 states per eV per formula unit cell, which is less than the one of nonmagnetic state ($=5.78$ states per eV per formula unit cell). The specific heats are evaluated as $0.84 \text{ mJ}/(\text{K}^2 \cdot \text{mol})$ and $6.86 \text{ mJ}/(\text{K}^2 \cdot \text{mol})$ for the collinear antiferromagnetic state and nonmagnetic state respectively, consistent with the specific heat measurement [20]. The paramagnetic susceptibility in the nonmagnetic state is about $1.18 \times 10^{-9} \text{ m}^3/\text{mol}$.

Fig. 4 shows the collinear antiferromagnetic electronic

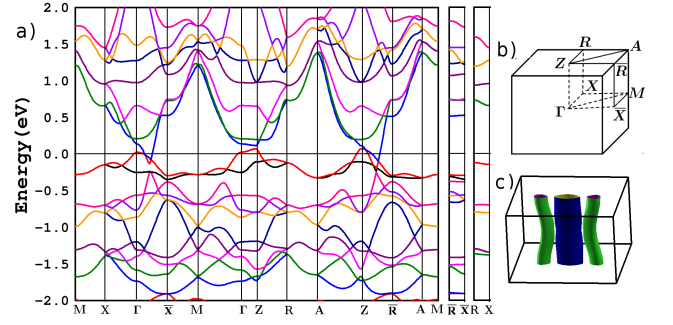


FIG. 4: (Color online) (a) The electronic band structure of LaFePO in the collinear antiferromagnetic state. The Fermi energy is set to zero. (b) The correspondent labels in Brillouin zone. (c) The Fermi surface sheets: a hole-type cylinder along ΓZ and two electron-type pockets between Γ and \bar{X} . ΓX corresponds to the parallel-aligned moment line and $\Gamma \bar{X}$ corresponds to the antiparallel-aligned moment line.

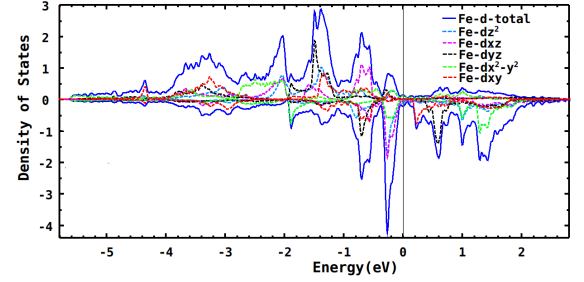


FIG. 5: (Color online) Calculated total and projected density of states at the five Fe-3d orbitals around one of the four Fe atoms in the collinear antiferromagnetic state unit cell. The Fermi energy is set to zero.

band structure and the Fermi surface. Unlike the ones in the nonmagnetic state [19], there are now only two bands crossing the Fermi level, one small hole cylinder along ΓZ and two small electron cylinders formed between Γ and \bar{X} . From the volumes enclosed by these Fermi surface sheets, we find that the hole carrier density is about $1.34 \times 10^{20}/\text{cm}^3$ and the electron carrier density is about $1.21 \times 10^{20}/\text{cm}^3$.

IV. ORIGIN OF THE MAGNETISM

By projecting the density of states onto the five 3d orbitals of Fe in the collinear antiferromagnetic state of LaFePO (Fig. 5), we find that the five up-spin orbitals are almost filled and the five down-spin orbitals are only partially filled. Moreover, the down-spin electrons are nearly uniformly distributed in these five 3d orbitals. This indicates that the crystal field splitting imposed by P atoms is relatively small and the Fe 3d-orbitals hybridize strongly with each other. As the Hund rule coupling is strong, this would lead to a magnetic moment formed around each Fe atom, as found in our

calculation. Actually, this is a universal feature for all iron pnictides, as we first found in LaFeAsO [6]. The polarization of Fe magnetic moments is thus due to the Hund's rule coupling.

In low temperatures, the Fe moments will interact with each other to form an antiferromagnetic ordered state. These ordered magnetic moments have been observed by elastic neutron scattering and other experiments in LaFeAsO and other pnictides[4, 11]. However, they are not exactly the moments obtained by the density functional theory (DFT) calculations, as we indicated first for LaFeAsO [6]. This is because the DFT calculation is done based on a small magnetic unit cell and the low-energy quantum spin fluctuations as well as their interactions with itinerant electrons are frozen by the finite excitation gap due to the finite-size effect. Thus the moment obtained by the DFT is the bare moment of each Fe ion. It should be larger than the ordered moment measured by the neutron scattering and other experiments. Our calculations show that the bare magnetic moment around each Fe atom is about $2\mu_B$. Moreover, the frustration between the J_1 and J_2 terms will further suppress the antiferromagnetic ordering at the two Fe-sublattices, each connected only by the J_2 terms. All of these together will reduce strongly the average magnetic ordered moment around each Fe measured by experiments, like the neutron scattering.

In high temperatures, there is no net static moment in the paramagnetic phase due to the thermal fluctuation, but the bare moment of each Fe ion can still be measured by a fast local probe like ESR (electron spin resonance). Recently the bare moment of Fe has been observed in the paramagnetic phase of BaFe₂As₂ by the ESR measurement [21]. The value of the moment detected by ESR is about $2.2 \sim 2.8 \mu_B$ in good agreement with our DFT result [6], which is but significantly larger than the ordered moment in the antiferromagnetic phase.

V. DISCUSSION IN CONNECTION WITH SUPERCONDUCTIVITY

As we see above, the next nearest neighbor antiferromagnetic superexchange interaction affects strongly the magnetic structure of the ground state. The magnetic fluctuation induced by the antiferromagnetic superexchange interactions should be responsible for the superconducting pairing. Upon doping, the long range ordering will be suppressed. However, we believe that the remanent antiferromagnetic fluctuation will survive, similar as in cuprate superconductors. We plot the superconducting critical temperatures T_c versus J_2 for the iron pnictide compounds with doping carriers or by applying high pressures in Fig. 6. As we see, the maximum critical temperatures T_c are in proportion to the next-nearest neighbor antiferromagnetic superexchange interaction J_2 . This suggests that there would exist an intrinsic relationship between the superconductivity and the

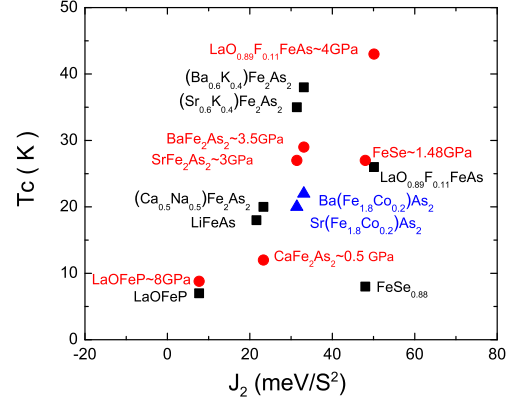


FIG. 6: Various critical superconductivity temperature T_c versus antiferromagnetic superexchange interaction J_2 for iron-based pnictides or chalcogenides with doping or under high pressures. T_c are taken from Refs. 1, 7–9, 22–30.

Pnictogen-bridged antiferromagnetic superexchange interactions.

The above analysis suggests that there are some similarities between pnictide and cuprate superconductors. Here we would also like to further address the difference between them is that the undoped cuprate is an antiferromagnetic Mott insulator while the undoped pnictide is an antiferromagnetic semimetal. In particular, in undoped pnictide there already coexist both local magnetic moments and itinerant electrons. This is similar as in the doped cuprate superconductors. In cuprate superconductors, the low-energy physics can be effectively described by the $t - J$ model, in which the coupling between local spins is the antiferromagnetic interaction and the doped holes or electrons can hop on the lattice.

For iron-based pnictides, the low energy spin dynamics can be approximately described by an antiferromagnetic Heisenberg model (Eq. (1) with the nearest and the next-nearest neighbor exchange interactions. However, the Fe spin (or magnetic moment) is not quantized since the electrons constituting the moment can propagate on the lattice, like in hole or electron doped high T_c superconductivity cuprates. Besides these superexchange interactions, the on-site Hund's rule coupling among different Fe 3d orbitals is important. This is because the crystal splitting of Fe 3d levels is very small and the spins of Fe 3d electrons are polarized mainly by this interaction. Thus we believe that the low-energy physical properties of these iron-based pnictides can be approximately described by the following effective Hamiltonian

$$H = \sum_{\langle ij \rangle, \alpha\beta} t_{ij}^{\alpha\beta} c_{i\alpha}^\dagger c_{j\beta} - J_H \sum_{i, \alpha \neq \beta} \vec{S}_{i\alpha} \cdot \vec{S}_{i\beta} + J_1 \sum_{\langle ij \rangle, \alpha\beta} \vec{S}_{i\alpha} \cdot \vec{S}_{j\beta} + J_2 \sum_{\langle\langle ij \rangle\rangle, \alpha\beta} \vec{S}_{i\alpha} \cdot \vec{S}_{j\beta}, \quad (2)$$

where $\langle ij \rangle$ and $\langle\langle ij \rangle\rangle$ represent the summation over the

nearest and the next-nearest neighbors, respectively. α and β are the indices of Fe 3d orbitals. $c_{i\alpha}^\dagger$ ($c_{i\alpha}$) is the electron creation (annihilation) operator.

$$\vec{S}_{i\alpha} = c_{i\alpha}^\dagger \frac{\vec{\sigma}}{2} c_{i\alpha} \quad (3)$$

is the spin operator of the α orbital at site i . The total spin operator at site i is defined by $\vec{S}_i = \sum_{\alpha} \vec{S}_{i\alpha}$. In Eq. (2), J_H is the on-site Hund's coupling among the five Fe 3d orbitals. The value of J_H is generally believed to be about 1 eV. $t_{ij}^{\alpha\beta}$ are the effective hopping integrals that can be determined from the electronic band structure in the nonmagnetic state[31]. It has been shown that the nearest and the next-nearest neighbor exchange coupling constants J_1 and J_2 in Eq. (2) can be calculated from the relative energies of the ferromagnetic, square antiferromagnetic, and collinear antiferromagnetic states with respect to the non-magnetic state. For the corresponding detailed calculations, please refer to the appendix in our paper in Ref. 6. Here we have assumed that the contribution of itinerant electrons to the energy is almost unchanged in different magnetically ordered states. Since the bare $t_{ij}^{\alpha\beta}$ and J_H can be considering independent of magnetic structures, the relative energies between different magnetic states are not affected by itinerant electrons.

VI. CONCLUSION

In conclusion, we have presented the first-principles calculation of the electronic structure of LaFePO. We find that like the situation in LaFeAsO, there are the next-nearest neighbor antiferromagnetic superexchange interactions bridged by P 3p-orbitals, which are much larger than the nearest neighbor ones. This gives rise to the collinear antiferromagnetic ordering of Fe spins in the ground state as observed in LaFeAsO by the neutron scattering. However, because of much smaller exchange interactions J_2 and J_1 in comparison with the ones in LaFeAsO, the corresponding transition temperatures should be very low in LaFePO, very likely less than 10K scaled according to LaFeAsO. This needs further experiment to test and verify. Based on the analysis of electronic and magnetic structures, we proposed that the low-energy physics of iron pnictides can be effectively described by the $t - J_H - J_1 - J_2$ model, defined by Eq. (2).

Acknowledgments

This work is supported by National Natural Science Foundation of China and by National Program for Basic Research of MOST, China.

-
- [1] Y. Kamihara, T. Watanabe, M. Hirano, and H. Hosono, *J. Am. Chem. Soc.* **130**, 3296 (2008).
 - [2] F. Ma and Z.Y. Lu, *Phys. Rev. B* **78**, 033111 (2008).
 - [3] F. Ma *et al.*, *Phys. Rev. Lett.* **102**, 177003 (2009).
 - [4] C. de la Cruz *et al.*, *Nature (London)* **453**, 899 (2008).
 - [5] S.L. Li *et al.*, *Phys. Rev. B* **79**, 054503 (2009).
 - [6] F. Ma, Z.Y. Lu, and T. Xiang, *Phys. Rev. B* **78**, 224517 (2008).
 - [7] M. Rotter *et al.*, *Phys. Rev. Lett.* **101**, 107006 (2008).
 - [8] X. C. Wang *et al.*, *Solid State Commun.* **148**, 538 (2008).
 - [9] F.-C. Hsu *et al.*, *Proc. Natl. Acad. Sci. U.S.A.* **105**, 14262 (2008).
 - [10] J. Dong *et al.*, *Europhys. Lett.* **83**, 27006 (2008).
 - [11] W. Bao *et al.*, *Phys. Rev. Lett.* **102**, 247001 (2009).
 - [12] I.I. Mazin, D.J. Singh, M.D. Johannes, and M.H. Du, *Phys. Rev. Lett.* **101**, 057003 (2008).
 - [13] T. Yildirim, *Phys. Rev. Lett.* **101**, 057010 (2008).
 - [14] Q. Si and E. Abrahams, *Phys. Rev. Lett.* **101**, 076401 (2008).
 - [15] P. Giannozzi *et al.*, <http://www.quantum-espresso.org>.
 - [16] J. P. Perdew, K. Burke, and M. Ernzerhof, *Phys. Rev. Lett.* **77**, 3865 (1996).
 - [17] D. Vanderbilt, *Phys. Rev. B* **41**, 7892 (1990).
 - [18] Renchao Che, Ruijuan Xiao, Chongyun Liang, Huaixin Yang, Chao Ma, Honglong Shi, and Jianqi Li, *Phys. Rev. B* **77**, 184518 (2008).
 - [19] S. Lebegue, *Phys. Rev. B* **75**, 035110 (2007).
 - [20] T. M. McQueen, M. Regalacio, A.J. Williams, Q. Huang, J.W. Lynn, Y.S. Hor, D.V. West, M.A. Green, and R.J. Cava, *Phys. Rev. B* **78**, 024521 (2008).
 - [21] T. Wu, J.J. Ying, G. Wu, R.H. Liu, Y. He, H. Chen, X.F. Wang, Y.L. Xie, Y.J. Yan, and X.H. Chen, *Phys. Rev. B* **79**, 115121 (2009).
 - [22] P. L. Alireza, J. Gillett, Y. T. C. Ko, S. E. Sebastian, and G. G. Lonzarich, *J. Phys.: Condens. Matter* **21**, 012208 (2009).
 - [23] H. Takahashi, K. Igawa, K. Arii, Y. Kamihara, M. Hirano, and H. Hosono, *Nature* **453**, 376 (2008).
 - [24] A. S. Sefat, R. Jin, M. A. McGuire, B. C. Sales, D. J. Singh, and D. Mandrus, *Phys. Rev. Lett.* **101**, 117004 (2008).
 - [25] A. Leithe-Jasper, W. Schnelle, C. Geibel, and H. Rosner, *Phys. Rev. Lett.* **101**, 207004 (2008).
 - [26] Y. Mizuguchi, F. Tomioka, S. Tsuda, T. Yamaguchi, and Y. Takano, *Appl. Phys. Lett.* **93**, 152505 (2008).
 - [27] G. F. Chen, Z. Li, J. Dong, G. Li, W. Z. Hu, X. D. Zhang, X. H. Song, P. Zheng, N. L. Wang, and J. L. Luo, *Phys. Rev. B* **78**, 224512 (2008).
 - [28] G. Wu, H. Chen, T. Wu, Y. L. Xie, Y. J. Yan, R. H. Liu, X. F. Wang, J. J. Ying, and X. H. Chen, *J. Phys.: Condens. Matter*, **20**, 422201 (2008).
 - [29] Y. Kamihara, H. Hiramatsu, M. Hirano, R. Kawamura, H. Yanagi, T. Kamiya, and H. Hosono, *J. Am. Chem. Soc.* **128**, 10012 (2006).
 - [30] K. Igawa, H. Okada, K. Arii, H. Takahashi, Y. Kamihara, M. Hirano, H. Hosono, S. Nakano, and T. Kikegawa, *J. Phys. Soc. Jpn.* **78**, 023701 (2009).
 - [31] C. Cao, P.J. Hirschfeld, and H.P. Cheng, *Phys. Rev. B* **77**, 220506(R) (2008).